Published in final edited form as:
Cell Stem Cell. 2010 October 8; 7(4): 483–495. doi:10.1016/j.stem.2010.08.014.

Microglia shape adult hippocampal neurogenesis through apoptosis-coupled phagocytosis

Amanda Sierra[1], **Juan M. Encinas**[1,2], **Juan JP Deudero**[1], **Jessica H. Chancey**[3], **Grigori Enikolopov**[2], **Linda S. Overstreet-Wadiche**[3], **Stella E. Tsirka**[4], and **Mirjana Maletic-Savatic**[1]

[1] Department of Pediatrics, Baylor College of Medicine, Houston, TX 77030

[2] Cold Spring Harbor Laboratory, Cold Spring Harbor, NY 11724

[3] Department of Neurobiology, University of Alabama at Birmingham, Birmingham, AL 35294

[4] Department of Pharmacology, Stony Brook University, Stony Brook, NY 11733

Summary

In the adult hippocampus, neuroprogenitor cells in the subgranular zone (SGZ) of the dentate gyrus give rise to newborn neuroblasts. However, only a small subset of these cells integrates into the hippocampal circuitry as mature neurons at the end of a four-week period. Here, we show that the majority of the newborn cells undergo death by apoptosis in the first one to four days of their life, during the transition from amplifying neuroprogenitors to neuroblasts. These apoptotic newborn cells are rapidly cleared out through phagocytosis by unchallenged microglia present in the adult SGZ niche. Phagocytosis by the microglia is efficient and undeterred by increased age or inflammatory challenge. Our results suggest that the main critical period of newborn cell survival occurs within a few days of birth and reveal a new role for microglia in maintaining the homeostasis of the baseline neurogenic cascade.

Introduction

Microglia are the brain immune cells, responsible for orchestrating the brain innate immune response. They belong to the monocytic-macrophage lineage (Ajami et al., 2007) and are therefore natural-born, professional phagocytes (Mallat et al., 2005). During development,

Contact information: Mirjana Maletic-Savatic. Baylor College of Medicine, Houston, TX 77030. Tel. 713 798 7340, Fax 713 798 4484, maletics@bcm.edu. Amanda Sierra. Baylor College of Medicine, Houston, TX 77030. Tel. 713 798 7340, Fax 713 798 4484, amanda.sierrasaavedra@gmail.com.

Author's contributions:
AS designed and performed the experiments, analyzed the data, and wrote the paper.
JME performed experiments
JJP performed experiments
JHC performed experiments
LSOW provided the POMC-EGFP mice and critically reviewed the paper
GE provided the nestin-GFP and the nestin-CFPNuc mice and critically reviewed the paper.
SET provided the fms-EGFP mice and critically reviewed the paper.
MMS designed and supervised all the experiments, and wrote the paper.

microglia play an essential role by phagocytosing the excess of neuroblasts, such as in the cerebellum (Marin-Teva et al., 2004). In the adult brain, microglia have been mostly studied in the context of disease, when they become activated or challenged by pathological conditions. Activated microglia are hypertrophic or amoeboid-like (Aloisi, 2005); they initiate an inflammatory response through the secretion of pro-inflammatory cytokines (Aloisi, 2005) and phagocytose dying cells (Kettenmann, 2007). Recently, it has been suggested that microglia play a role in adult neurogenesis, such as when activated by inflammation (Butovsky et al., 2006; Ekdahl et al., 2003a; Monje et al., 2003) or by adrenalectomy (Battista et al., 2006), or when neurogenesis was induced by enriched environment (Ziv et al., 2006). However, the potential role of microglia in adult neurogenesis in normal conditions remains unknown.

One of the important issues in neurogenesis, both during development and in the adult brain, is the survival of the newborn cells. In the subgranular zone (SGZ) of the dentate gyrus, where neurogenesis occurs throughout adulthood, only a few newborn cells are incorporated into the circuitry, and the majority of them are presumed to die at the immature neuron stage (Ma et al., 2009). However, a sharp decline in the number of newborn cells, labeled with the thymidine analog 5-bromo-2'-deoxyuridine (BrdU), occurs much earlier (Kempermann et al., 2004; Kronenberg et al., 2003; Mandyam et al., 2007). Furthermore, it has not been firmly established that this decline in the number of the BrdU immunopositive cells is due to apoptosis. Apoptosis of newborn cells is hard to evaluate and initial studies provided only qualitative evidence (Biebl et al., 2000; Dayer et al., 2003; Kuhn et al., 2005). As the cell survival is essential for regulation of the neurogenic cascade, we sought to define the critical period of survival of newborn cells in the adult hippocampus and the clearing mechanism that removes the apoptotic debris.

Based on published data of BrdU decay (Kempermann et al., 2004; Kronenberg et al., 2003; Mandyam et al., 2007), we hypothesized that newborn cells undergo apoptosis mostly during an early critical period and that the apoptotic debris is removed from the SGZ neurogenic niche by microglia. In most tissues, apoptotic cells are phagocytosed within 1–2 hrs from the start of apoptosis (Savill, 1997). Thus, if microglial phagocytosis in the healthy adult brain is similarly rapid, the probability of detecting apoptotic newborn cells would be low, explaining the difficulty in obtaining quantitative data on apoptosis and phagocytosis. Herein, we addressed this issue by investigating phagocytosis of the apoptotic cells in the healthy SGZ neurogenic niche, performed by “unchallenged” microglia. The unchallenged microglia we refer to are ramified microglia in normal conditions, where there are no exogenous challenges, but only the local signals regulating their behavior and function.

We found that unchallenged microglia are indeed an essential component of the normal hippocampal neurogenic niche and are involved in phagocytosing apoptotic newborn cells. In addition, we show that the main critical period of survival of young adult SGZ newborn cells occurs early in the cell life, during the transition from late amplifying neuroprogenitors (ANPs) to neuroblasts (NBs). Our data suggest that apoptosis in the first four days of cell life followed by microglial phagocytosis accounts for the decay in the number of newborn cells in the young adult SGZ and provide a new role for unchallenged microglia in adult neurogenesis.

Results

Apoptosis is coupled to phagocytosis in the young adult SGZ

We first analyzed the distribution of apoptotic cells within the hippocampal neurogenic niche, in the young adult (1-month-old (m.o.)) mouse (Fig. 1A, B). Apoptosis is characterized by specific nuclear morphology such as pyknosis (DNA condensation) and karyorrhexis (nuclear fragmentation), both detected by condensed staining with DAPI, a DNA dye (Savill et al., 2002) (Fig. 1A). Pyknotic nuclei are clearly distinguished from the nuclei of other healthy cells, such as neuronal (with puncta of bright heterochromatin), and endothelial (crescent shape), as well as from cells in mitosis (in which the separating chromosomes can be observed) (Fig. S1). In addition, apoptosis is functionally characterized by activation of caspase 3 (act-casp3) (Nicholson et al., 1995), which cleaves β-actin, resulting in a fragment called fractin (Yang et al., 1998) (Fig. 1A; Fig. S1). In the young adult SGZ, 100% of the cells labeled with anti-act-casp3 antibody (181/181 cells, n=5) or fractin antibody (151/151 cells, n=3) are also identified as pyknotic. More than 90% of the apoptotic cells (pyknotic/karyorrhectic, act-casp3+) are located strictly in the SGZ (Fig. 1A, B), defined as a layer of cells expanding 5μm into the hilus and 15μm into the granular cell layer. Apoptotic cells are rarely found in the hilus, granular, or molecular layers (Fig. 1A, B), as reported (Biebl et al., 2000). The abundance of apoptotic cells within the SGZ neurogenic niche suggests their relationship with the neurogenic cascade (Biebl et al., 2000), and herein we investigate their identity and the clearing mechanism.

We hypothesized that the apoptotic cells in the normal young adult SGZ were removed through phagocytosis performed by resident microglia. To identify microglia, we used immunofluorescent labeling with an antibody against Iba-1 (ionized calcium binding adaptor molecule 1, a marker of the macrophage lineage) in wild type animals or transgenic fms-EGFP mice (in which the regulatory elements of the macrophage colony stimulating factor receptor gene drive EGFP expression), where EGFP is expressed by microglia (Sierra et al., 2007). Iba1 and EGFP are both expressed throughout the cytoplasm, and thus outline both the cell body and the processes of microglia. The relationship between the apoptotic profiles and microglia in the normal young adult SGZ can be classified into three main categories: not-phagocytosed, early phagocytosis, or late phagocytosis (Fig. 1C; Fig. S1). Some pyknotic cells labeled with act-casp3 were not in the vicinity of a microglial cell (Fig. 1C1; *not-phagocytosed*), whereas others were being approached by a microglial process (Fig. S1D1). In other instances, apoptotic cells were completely engulfed by microglia (Fig. 1C2), had conspicuous act-casp3 labeling and a loose, patchily stained microglial phagocytic pouch, suggesting that phagocytosis was recently initiated (*early phagocytosis*). Another category of cells showed faint act-casp3 labeling and a tight microglial pouch, indicating that phagocytosis was almost complete (Fig. 1C3; *late phagocytosis*). Occasionally, puncta of act-casp3 were seen within the microglial processes and diminutive DAPI or BrdU particles within a microglial pouch (Fig. S1), appearing to be in the *terminal stages* of phagocytosis.

The efficiency of the microglial phagocytosis is determined by the phagocytic index (Ph-index), the percentage of the apoptotic cells undergoing microglial phagocytosis (early and

late phagocytosis combined). In the adult SGZ, microglia phagocytose 91.0 ± 3.1% of the pyknotic cells (266/287 cells, n=10 wild type mice); 91.6 ± 3.5% of the pyknotic, act-casp3 immunoreactive cells (169/181 cells, n=5 fms-EGFP mice); and 94.4 ± 2.4% of the pyknotic, fractin immunoreactive cells (143/151 cells, n=3 fms-EGFP mice) (Fig. 1D; Table S1). There are no significant differences in the Ph-index (ANOVA, p=0.815) among the three methods used for detecting apoptosis. The remaining 5–8% of apoptotic cells not phagocytosed by microglia were always in the earliest stages of apoptosis (large pyknotic body, high expression of act-casp3 or fractin; Fig. 1C1; Fig. S1), suggesting that the phagocytic process has not yet begun.

Phagocytosis of the apoptotic cells is performed by ramified microglia in the SGZ neurogenic niche, where their processes intermingle among quiescent and amplifying neuroprogenitors (NPCs) and neuroblasts (NBs) (Fig. 1E). NPCs were visualized in nestin-GFP transgenic mice which express GFP under the nestin promoter and regulatory elements (Mignone et al., 2004). NBs were visualized by immunolabeling with an antibody raised against PSA-NCAM, the polysialated form of the neural cell adhesion molecule, expressed in migrating newborn cells committed to the neuronal fate. To determine the extent of the microglial presence in the niche, we quantified the percentage of NPCs and NBs contacted by microglia (Fig. S2). Approximately one-third (37 ± 4%) of the NPCs and 30 ± 3% of the NBs are in contact with microglial processes (n=4). In the majority of cases, the contacts are tangential, and only occasionally, the microglial cell body is apposed to the NPCs or NBs cell body (Fig. S2). These data indicate a complex spatial relationship between NPCs/NBs and microglia, and provide the anatomical support for our hypothesis that unchallenged microglia efficiently phagocytose newborn cells in the normal adult SGZ.

Unchallenged microglia phagocytose apoptotic cells in the normal adult SGZ

The phagocytic microglia shows ramified morphology typical of unchallenged microglia. To further confirm this observation, we tested the expression of two markers which increase upon microglial activation: CD11b (integrin α M) and CD68 (macrosialin) (Ekdahl et al., 2003a). Their expression in SGZ phagocytic microglia was compared to their expression in non-phagocytic microglia from the CA2 hippocampal region, as a negative control (Fig. 2A, Fig. S2). As a positive control, we analyzed their expression in SGZ microglia of animals treated with bacterial lipopolysaccharides (LPS) (Fig. 2A, S3), which induce an inflammatory challenge and activate microglia (Sierra et al., 2007). The expression of markers in SGZ phagocytic microglia (CD11b-low, CD68-low) is similar to that of CA2 non-phagocytic microglia and dramatically different from that of microglia challenged with LPS (CD11b-high, CD68-high) (Fig. 2A, Fig. S2). This data thus suggest that phagocytosis does not activate microglia the same way an inflammatory challenge does, providing functional evidence that SGZ microglia phagocytosing apoptotic cells in physiological conditions are indeed unchallenged.

Phagocytosis by unchallenged microglia occurs by a special modification of the microglial processes, which form a phagocytic pouch that engulfs the apoptotic cell, as shown by volume rendering of phagocytic SGZ microglia in confocal z-stacks (Fig. 2B). The phagocytic pouches take on a ball-and-chain structure connected with the microglial cell

body at a terminal or *en passant* branch (Fig. 2B), clearly distinguishable from the microglial body. Finally, the phagocytosis of apoptotic cells by microglia in the normal young adult SGZ is also observed at the ultrastructural level (Fig. 2C). Microglial processes were labeled with antibodies against Iba1 and revealed by peroxidase staining. Two examples of pyknotic nuclei engulfed by microglial processes in the SGZ are shown in Fig. 2C. Taken together, the above results indicate that unchallenged microglia are largely responsible for recognizing and eliminating apoptotic cells in the young adult SGZ during healthy conditions.

Identity of the phagocytosed apoptotic cells

To determine the cellular identity of the apoptotic cells being phagocytosed by microglia, we utilized antibodies for most of the cell types present in the SGZ (Fig. 3; Fig. S3, Table S2). We find that 8 ± 4% of the total number of apoptotic cells are only nestin-GFP+; 42 ± 11% are only PSA-NCAM+; and 17 ± 4% express both nestin-GFP and PSA-NCAM (n=4 mice). 28 ± 6% of the apoptotic cells express POMC-EGFP, a marker of postmitotic differentiating newborn neurons (Overstreet et al., 2004) (n=6 mice), while none express doublecortin, a marker of NBs (DCX; n=6 mice). None of the SGZ apoptotic cells express NeuN (a marker of immature and mature neurons) and only 5% dimly express Prox1 (a specific marker of granule cells expressed in early stages of neuronal differentiation) (n=3 mice). In addition, no apoptotic astrocytes or quiescent NPCs were observed using hGFAP-GFP transgenic mice (n=4 mice), in which EGFP is expressed under the control of the human GFAP promoter (Glial Fibrillary Acidic Protein) (Zhuo et al., 1997). We, however, observed a small percentage of apoptotic endothelial cells (4% ± 2%), labeled with PECAM1 (n=4 mice). Finally, no apoptotic cells express Myelin Binding Protein (MBP), a marker of oligodendrocytes (n=3 mice), or GFAP using an anti-GFAP antibody (n=3 mice). We also did not observe apoptotic cells being engulfed by GFAP+ or hGFAP-GFP+ astrocytes. Thus, albeit astrocytes have been implicated in the phagocytosis of synaptic membranes during synaptic remodeling (Aldskogius et al., 1999), our results exclude them from playing a significant role in phagocytosing apoptotic cells in the normal young adult SGZ.

Interestingly, up to 32 ± 5% (n=4 nestin-GFP mice) of the apoptotic profiles could not be identified with any of the markers we used. The majority (79 ± 10%) of these unidentified cells are strictly located within the physical niche formed by nestin-GFP+ NPC processes, as well as POMC-EGFP+ NB processes (Fig. S3), suggesting their relationship with the neurogenic cascade despite their lack of immunolabeling with the tested biomarkers. Nonetheless, the expression of biomarkers in apoptotic cells should be taken cautiously, since our ability to detect them depends on the expression levels of the protein or the transgene and their rate of degradation, both internally by caspases or externally by microglia. Overall, our results suggest that the majority of the apoptotic cells in the normal young adult SGZ are part of the neurogenic cascade and belong to a transitional stage between late ANPs and early NBs.

Newborn cells undergo early apoptosis

The number of BrdU-labeled newborn cells in the SGZ declines dramatically during the first week of their life (Kempermann et al., 2004; Kronenberg et al., 2003; Mandyam et al., 2007). Based on our data (Fig. 3), we hypothesized that this decline is due to apoptosis of newborn cells, and we tested it in a BrdU pulse-and-chase experiment. One-month-old mice received a single dose of BrdU (250mg/kg) and were sacrificed at different time points (n=3–4 mice per time point; Fig. 4A). We analyzed the cell birth date by BrdU labeling and apoptosis by nuclear morphology (Fig. 4B–E). We quantified the number of newborn cells (BrdU immunopositive (BrdU+)), the total number of apoptotic cells (pyknotic), and the number of newborn apoptotic cells (BrdU+ pyknotic) in confocal z-stacks, and then calculated the number of those cells over the volume spanned by the SGZ per hippocampus.

The number of *BrdU+* cells reaches a peak at 2 days post-injection (dpi), decaying exponentially afterwards (R^2=0.888, p<0.0001; Fig. 4B), in agreement with previous observations (Kempermann et al., 2004; Kronenberg et al., 2003; Mandyam et al., 2007). The decay is faster during 2 - 4dpi (47–69 BrdU+ cells lost per hour, i.e., 0.8–1.0 % of the 2dpi-BrdU+ cells per hour) and slower during 8–15dpi (0–11 BrdU+ cells lost per hour, i.e., 0–0.2 % of the 2dpi-BrdU+ cells per hour) (Fig. 4C). After 15dpi, no significant drop in the number of BrdU+ cells is detected (p>0.05, Fig. 4B). The first *apoptotic BrdU+* cells appear 24h after the BrdU administration and peak at 2dpi (121 ± 33 cells/hippocampus), accounting for 7.6 ± 3% of the total number of apoptotic cells and 2.2 ± 0.8% of the total number of BrdU+ cells at that time point (Fig. 4D,E; Table S3). These data provide evidence that newborn cells undergo apoptosis, as the time course of apoptotic BrdU+ cells parallels the decline of the BrdU+ cells. Yet, despite the apparent match, the number of apoptotic SGZ cells labeled with BrdU is strikingly low, compared to the total number of apoptotic cells in the SGZ (Fig. 4D). One possible explanation is that the decrement in the number of BrdU+ cells is due to BrdU dilution or alternatively, that a single pulse of BrdU, which circulates approximately 15min (Mandyam et al., 2007), labels a fraction of the dividing NPCs population, thus decreasing the probability of detection of newborn apoptotic cells.

To explore those two scenarios, we utilized a cumulative, BrdU-saturating paradigm that consisted of repeated injections of BrdU every 3h for a 24h period, as previously reported (Hayes and Nowakowski, 2002) (n=3–4 mice per time point; Fig. 5A). This approach allowed us to label the majority of the cohorts of dividing cells over a 24h period and to re-label each cohort two to three times (as the estimated duration of the S phase is approximately 8h (Hayes and Nowakowski, 2002)). This labeling paradigm does not affect the number of apoptotic cells, which remains stable regardless of the number of injections (Fig. S4).

Using the cumulative BrdU labeling paradigm, we again observed the decay in the number of newborn *BrdU+* cells in the young adult SGZ (Fig. 5B). The maximum number of BrdU+ cells is detected at the first time point studied, 27hrs post-injection (1.1dpi), after which the number of BrdU+ cells declines at an exponential rate (R^2=0.758, p<0.0001). After 8dpi, no significant decline of BrdU+ cells is observed (p>0.05) (Fig. 5B). Interestingly, the rate of the BrdU+ cell decline per hour is different at different time points. Initially, during the first

2dpi, the decline occurs at a rate of 400 BrdU+ cells per hour (2% of the 1.1dpi-BrdU+ cells per hour), and then it drops to 20–80 BrdU+ cells per hour between 4 and 8dpi (0.1–0.4% of the 1.1dpi-BrdU+ cells per hour) (Fig. 5C). *Apoptotic BrdU+* cells are detected throughout the time course and are often located in clusters of dividing cells, particularly at 2dpi (Fig. 5D, Fig. S4). The apoptotic BrdU+ ratio is maximal between 2dpi and 4dpi, when 32–33% of the apoptotic cells are labeled with BrdU (460 ± 101 and 532 ± 19 apoptotic BrdU+ cells per hippocampus at 2dpi and 4dpi, respectively) (Fig. 5D; Fig. S4; Table S4). As in the single BrdU labeling experiment, the BrdU+ decay (Fig. 5C) parallels the apoptotic BrdU+ fraction (Fig. 5D) along the time course of the cumulative BrdU labeling experiment. These data demonstrate that the majority of the apoptotic cells in the young adult SGZ are newborn cells, the bulk of which are only 1–4 days old when undergoing apoptosis.

Surprisingly, the apoptotic BrdU+ cells represent only 3.9 ± 0.1 to 6.0 ± 0.0 of the total BrdU+ cells at their maximum (2 and 4dpi, respectively) in the cumulative paradigm as well. Since the decay rates in the single and cumulative labeling paradigms are similar (Fig. 4C and 5C), a major contribution of BrdU dilution to the decline in the number of cells can be ruled out. Thus, the low percentage of apoptotic BrdU+ cells compared to the total number of BrdU+ cells suggests that these cells are rapidly removed from the neurogenic niche, rendering them difficult to detect and quantify. Our estimation (see Methods), based on the analysis of the decay between two consecutive time points, indicates that the clearance time is 1.2–1.5h per apoptotic cell (at 1.1–1.4dpi and 1.4–2dpi, respectively). At those time points, 92–95% of the apoptotic cells are located in the SGZ, and only 5–8% in the hilus, therefore suggesting that the apoptotic newborn cells are not displaced, but rather phagocytosed locally (Fig. S4). Thus, the combination of a high phagocytic index (about 91%, Fig. 1D) and a short clearance time suggests that microglia are very efficient in removing the apoptotic corpses from the young adult SGZ neurogenic niche.

Taken together, the above results indicate that the major stage of culling of newborn cells in the young adult SGZ occurs during the first 1–4 days of cell life, when 56% of the newborn cells are lost, the decay rate is high (400 cells/hr) and a high percentage of apoptotic cells are BrdU+ (10–33%). From 4 to 8 days of cell life, another 25% of the newborn cells are lost; the decay rate is low (20–80 cells/hr) and a low percentage of apoptotic cells are BrdU+ (6–8%). The second period of apoptosis could represent the decaying tail of the first apoptotic period, or it might represent a second wave of culling. After 11dpi, no further loss of BrdU+ cells is detected, although occasional apoptotic BrdU+ cells are found. Given the rate of the decay and the labeling of apoptotic cells with BrdU, it thus appears that the main critical period for survival of the newborn cells during young adult neurogenesis occurs within 4 days of cell birth.

To further explore the differences between the two critical periods, we analyzed the expression of two markers, nestin-GFP and POMC-EGFP, at 3dpi and 8dpi, using the cumulative BrdU labeling paradigm (Fig. 5E, F; Fig. S4). In the early critical period (3dpi), 28 ± 5% of the apoptotic BrdU+ cells express nestin-GFP (12/42 apoptotic BrdU+ cells, n=4 mice) and 8 ± 2% express POMC-EGFP (3/42 apoptotic BrdU+ cells, n=3 mice), confirming our previous observation that in this period, the cells undergoing apoptosis are in transition between ANPs (Nestin-GFP+) and NBs (POMC-EGFP+). In the late critical

period (8dpi), none of the apoptotic BrdU+ cells express nestin-GFP (0/3 apoptotic BrdU+ cells, n=3 mice) and 88 ± 13% express POMC-EGFP (5/6 apoptotic BrdU+ cells, n=3 mice), indicating that more differentiated NBs undergo apoptosis during this critical period of survival.

Microglial phagocytic activity is preserved despite the age-induced decrease of neurogenesis

During aging, there is a well-reported decrease in hippocampal neurogenesis largely attributable to decreased proliferation (Kuhn et al., 1996). We therefore asked what happens with apoptosis with increased age and whether the coupling between apoptosis and phagocytosis in the adult SGZ persists during age-induced decrease in neurogenesis. As we have shown, the majority of the apoptotic cells in the young adult SGZ are 1–4 days old and express biomarkers of late ANPs/early NBs (Figs. 3–5). Our data, thus, predict a decrease in the number of apoptotic cells in parallel with the decrease in SGZ neurogenesis and concomitantly with the increased age.

We analyzed both apoptosis and phagocytosis in the SGZ at 1, 2, 5 and 12m.o. (Fig. 6; n=4 mice). Apoptotic cells were identified based on pyknosis, NBs with PSA-NCAM, and microglia with Iba1. As expected, the number of PSA-NCAM + NBs as well as the number of apoptotic cells in the SGZ decreases during adulthood (Fig. 6A, B). Importantly, the Ph-index remains constant in the ages studied (around 92%; Fig. 6C; Table S5), indicating that the microglial phagocytic activity is preserved throughout adulthood. Interestingly, aging results in chronic activation of microglia with increased production of pro-inflammatory cytokines (Sierra et al., 2007). Even though we have not analyzed the amount of cytokines produced by microglia in our experiments, our data imply that throughout adulthood microglia are equally efficient in phagocytosing apoptotic cells in the SGZ neurogenic niche.

Microglial phagocytic activity is preserved during acute neuroinflammation

Finally, we investigated whether an exogenous inflammatory challenge known to activate the microglial inflammatory response interfered with the SGZ phagocytosis. We induced acute neuroinflammation by peripheral administration of LPS (1 mg/kg), which stimulates microglia to express pro-inflammatory cytokines that peak at 3h and return to basal levels by 24h (Sierra et al., 2007). Two independent experiments were done to test the short (8h) or long (22h) effect of LPS (Fig. 7; n=4–5 mice per group). To test the effect of the LPS on survival, animals were injected with iodo-deoxyuridine (IdU; 42.5mg/kg) two days prior to the administration of LPS or vehicle (Fig. 7A). To test the effect of the LPS on NPC proliferation, animals were injected with chloro-deoxyuridine (CldU; 57.5mg/kg) 2h prior to sacrifice. We assessed the number of IdU+ and CldU+ cells (by immunolabeling), apoptosis (by nuclear morphology), and microglial engulfment (by Iba1 immunolabeling).

No significant changes in NPC proliferation were observed, either 8 or 22h after the LPS treatment, but we noted a significant decrease in the survival of 2-day-old IdU+ cells 22h after the LPS in the treated compared to control animals (40 ± 13% decrease; p=0.0326, Student-t test; Fig. 7B,C; Fig. S5). The decreased survival is most likely the result of

increased apoptosis early on, since in LPS-treated animals 8h thereafter, we find a 242 ± 44% increase in apoptotic cells compared to control animals (p=0.0166, Student t-test). LPS, either after 8h or 22h, failed to induce any detectable proliferation of microglia (data not shown). Thus, the increased number of apoptotic cells 8hr after the LPS is cleared out by the same number of microglial cells, and we frequently detected microglia phagocytosing several apoptotic cells (Fig. 7C3). We calculated that the phagocytic capacity, i.e., the percentage of microglia with multiple (0–4) phagocytic profiles, increases 2.41 times in LPS-treated vs. control mice, 8h after the administration of LPS (Fig. 7C4). In control mice, microglia has in average 0.35 phagocytic profiles per cell, and the majority of them has none or one profile; whereas 8h after the LPS, microglia has an average of 0.84 phagocytic profiles per cell, and a significant percentage shows more than one phagocytic profile per microglial cell (Fig. 7C4). Remarkably, either 8 or 22h after the LPS, the Ph-index remains constant and around 90–96% (Fig. 7B; Table S6). Thus, these results indicate that the phagocytic efficiency of microglia in the young adult SGZ is not perturbed during acute inflammatory challenge.

Discussion

In the present study, we reveal novel properties of the cellular niche that modulates young adult hippocampal neurogenesis. First, we find that the decay in the number of newborn cells in the young adult SGZ is due to apoptosis of newborn cells. Second, the majority of apoptosis occurs within the first 1–4 days of cell birth during the transition from late ANPs to early NBs, suggesting that the main critical period for newborn cell survival occurs very early in neurogenesis, in contrast to the generalized assumption that survival is regulated at the immature neuron stage (Ma et al., 2009). Third, phagocytosis of the apoptotic newborn cells is performed exclusively by “unchallenged” microglia, indicating a novel, previously un-recognized role of such microglia in the normal adult SGZ neurogenic niche which has not been acknowledged in recent reviews (Ekdahl et al., 2009; Neumann et al., 2009). Phagocytosis itself does not appear to activate microglia in the same way an inflammatory challenge does, contrary to the widespread view that activation is a pre-requisite for phagocytosis (Kettenmann, 2007). Phagocytosis by unchallenged microglia involves the processes rather than the cell body and is highly efficient, as measured by the clearance time, the Ph-index and the phagocytic capacity. Microglial efficiency remains the same during adulthood and acute inflammation, suggesting the importance of phagocytosis for the maintenance of the functional neurogenic niche in both health and disease.

The majority of newborn cells undergo apoptosis

The disappearance of BrdU-labeled newborn cells in the adult SGZ, particularly in the first week of cell life, was first described by Kronenberg and collaborators (Kronenberg et al., 2003) and has been shown by many others (Kempermann et al., 2004; Mandyam et al., 2007). The decay of newborn cells after the first week of life has also been observed using retroviral labeling of the progeny of SGZ dividing cells (Tashiro et al., 2006), but the early survival in such experiments has not been reported, as the expression of the genes delivered by viral vectors generally takes several days (Zhao et al., 2006). In contrast, genetic methods of labeling, using a nestin-CreER promoter, showed an accumulation of newborn cells

(Lagace et al., 2007). Because this later method labels all nestin-expressing cells and their progeny, not only the dividing ones, labeled cells accumulate as new progenitors are recruited to the pool of dividing cells. Therefore, to explain the decay of BrdU–labeled cells, two alternative explanations have been proposed, namely, dilution of the BrdU labeling by continuous NPC proliferation or death of the newborn cells. Mathematical models disputed the BrdU dilution hypothesis, showing that cell death has to occur in the first 72h to explain the discrepancy between the expected and the actual number of BrdU+ cells in the adult hippocampus, when using a saturating BrdU labeling paradigm (Hayes and Nowakowski, 2002). The prevailing view thus has been that SGZ newborn cells die by apoptosis at the immature neuron stage (reviewed in (Ma et al., 2009)). This assumption is based on the higher density of apoptotic cells in neurogenic areas, including the SGZ, compared to the rest of the brain (Biebl et al., 2000; Dayer et al., 2003; Kuhn et al., 2005), as well as on occasional, non-quantified colocalization of apoptotic markers with BrdU in the adult SGZ (Dayer et al., 2003; Mandyam et al., 2007). More recently, it was shown that constitutive overexpression of the anti-apoptotic protein Bcl-2 (Kuhn et al., 2005) or constitutive deletion of the pro-apoptotic gene Bax (Sun et al., 2004) increased SGZ neurogenesis, although these studies could not discriminate between embryonic vs. adult effects. Taken together, the published data has not compellingly demonstrated the identity or the age of the apoptotic cells in the adult SGZ neurogenic niche.

Herein, we provide evidence that the majority of young adult SGZ newborn cells undergo apoptosis soon after they are born. By comparing the decay rate of BrdU+ cells in the single and the cumulative BrdU labeling paradigms along the 1-month long time course, we exclude BrdU dilution as a major contributor to the BrdU decay. More importantly, we provide direct evidence of newborn cell apoptosis. The vast majority of apoptotic cells in the young adult SGZ are newborn cells, since they are labeled with BrdU along the time course of the cumulative paradigm. In addition, there is a conspicuous parallel between the BrdU+ decay rate and the apoptotic BrdU+ fraction along the evaluated time period, both in the cumulative and the single BrdU labeling paradigms. Notably, apoptosis is not an artifact of the BrdU labeling, as the number of SGZ apoptotic cells remains unchanged in control *vs.* BrdU-treated animals (both single and cumulative experiments). Finally, our data predict that if apoptotic cells in the adult SGZ are newborn cells, then rates of SGZ apoptosis should parallel the proliferation rates, at least in experimental paradigms where survival is not affected. In agreement with this prediction, we find that with increased age, which causes a well-known decrease in NPC proliferation (Kuhn et al., 1996), there is a significant decrease in the number of SGZ apoptotic cells. All these lines of evidence strongly suggest that the decay in the number of newborn cells labeled with BrdU can be explained by the apoptosis of the newborn cells.

The main critical period of survival of newborn cells occurs early in cell life

Our study also demonstrates that the critical period of survival of young adult SZG newborn cells occurs soon after cell division, during the first four days of cell life as they transit from late, proliferating ANPs to early, post-proliferative NBs. Adult SGZ newborn cell survival has usually been studied at 2–4 weeks of cell life, at the late NBs or immature neuron stages, when it is known to be affected by animal behavior, neuronal activity, growth factors, drugs

of abuse, and hormones (Ma et al., 2009). For instance, it has been suggested that NMDA receptor-dependent integration of the newborn neurons into the hippocampal circuitry determines the newborn cell survival in the third week of a cell life (Tashiro et al., 2006). In agreement, we observe apoptotic cells labeled with BrdU up to three weeks after BrdU injection, even though the number of apoptotic cells we detect at this time is small. Nonetheless, taking together our results and the published literature, it is likely that there are two critical periods for newborn cell survival in the young adult SGZ: a main, early critical period (1–4 days after cell birth), and a secondary, late critical period (1–3 weeks after cell birth). A similar scenario could also occur in the other adult neurogenic system, in which neural precursors residing in the subventricular zone give rise to NBs that migrate through the rostral migratory stream (RMS) towards the olfactory bulb (OB), where they differentiate into mature neurons and integrate into the circuitry. Apoptosis has been observed in the RMS as well as the OB (Petreanu and Alvarez-Buylla, 2002), perhaps representing the early (RMS) and late (OB) critical periods of survival. Similarly, an early critical period of survival is known to occur during the embryonic brain development, when up to 70% of embryonic neuronal precursors undergo cell death early after cell birth, independent of target innervation (Thomaidou et al., 1997). However, the mechanisms regulating this early survival as well as the clearance of apoptotic cells in the developing brain are not completely understood (de la Rosa and de Pablo, 2000). We speculate that, since cell death occurs while the cells are still in a highly proliferative stage, apoptosis and mitosis could be functionally related. In fact, it has been recently shown that during asymmetric NB division in *C. elegans*, the same cellular machinery is responsible for both the orientation of the cleavage plane during cell division and the induction of apoptosis (Hatzold and Conradt, 2008). Thus, the early apoptosis of newborn cells in the young adult SGZ may be due to an evolutionarily conserved mechanism related to the mitosis of neural precursors.

The pruning of adult newborn cells during an early critical period of survival is a physiological mechanism whose occurrence in disease conditions remains to be studied. For instance, seizures induce widespread necrosis and apoptosis of neurons (Weise et al., 2005) as well as apoptosis of newborn cells within the neurogenic niche (Ekdahl et al., 2001; Ekdahl et al., 2002; Ekdahl et al., 2003b). However, it remains unknown which cell types within the neurogenic niche undergo seizure-induced apoptosis. We speculate that newborn cells in different stages of maturation may have different susceptibilities to seizure-induced apoptosis depending on the expression of glutamatergic receptors, which are largely responsible for the seizure activity (Eid et al., 2008). In the adult neurogenic niche, glutamate receptors are not expressed until the immature neuron stage, coinciding with the development of functional synaptic input (Nacher and McEwen, 2006). It is therefore possible that seizure-induced apoptosis affects more mature newborn cells than the processes leading to apoptosis of newborn cells in physiological conditions.

A novel role for microglia in the adult neurogenic niche

Our results also demonstrate that shortly after undergoing apoptosis, the SGZ newborn cells are phagocytosed and cleared out by unchallenged microglia. Phagocytosis by macrophages or activated, amoeboid microglia has been well-documented and is thought to occur in

response to pathological events (Kettenmann, 2007). In contrast, we herein show that in the normal adult brain, phagocytosis is carried out by unchallenged microglia, which show ramified morphology and have low expression of markers typically associated with inflammatory challenge, such as CD11b and CD68. Further, phagocytosis by unchallenged microglia takes place through terminal or *en passant* branches independent from the cell body. Microglial cells are present in the normal hippocampal neurogenic niche and sample it mostly through their processes, known to be highly motile (Davalos et al., 2005). Importantly, contact by microglia does not appear to be essential for the induction of apoptosis in the adult SGZ, since we consistently find a proportion of apoptotic cells that are not engulfed. This observation does not exclude a possible extrinsic influence of microglia on apoptosis, as has been shown to occur during development (Neumann et al., 2009).

Furthermore, our data suggest that phagocytosis by SGZ microglia is efficient, as measured by the clearance time, Ph-index and phagocytic capacity, thus providing the first quantified study of microglial phagocytosis in the adult brain. We estimate that the clearance time is 1.2–1.5 hr per apoptotic cell. This estimation is close to the range of estimated microglial clearance time *in vitro* (0.5–1.3hr) (Petersen and Dailey, 2004) and the clearance time in the developing cortex (2–3hr) (Thomaidou et al., 1997). Microglia also have a high Ph-index (about 91–94%), another indirect measure of their phagocytic efficiency. The Ph-index remains constant (> 90%) throughout normal neurogenesis as well as during adulthood and acute neuroinflammation. Thus, the combination of a high phagocytic index and a short clearance time suggests that microglia are very efficient in removing the apoptotic corpses from the adult SGZ neurogenic niche. The high phagocytic efficiency of microglia explains the difficulty in detecting and quantifying SGZ cells undergoing apoptosis. More importantly, the preservation of the Ph-index suggests a critical role of microglial phagocytosis in the maintenance of the neurogenic cascade, since it prevents primary apoptotic cells from undergoing secondary necrosis, with the consequent spillage of cellular contents leading to an inflammatory response (Savill et al., 2002), detrimental for neurogenesis (Ekdahl et al., 2003a; Monje et al., 2003).

In conclusion, we have shown that unchallenged microglia are an important component of the cellular neurogenic niche in the SGZ of the adult hippocampus. Previous reports had indicated either beneficial or detrimental effects of activated microglia on SGZ neurogenesis, depending on the particular paradigm of activation studied (Ekdahl et al., 2009). Initial reports suggested that inflammation, due to activation of microglia by irradiation or administration of high doses of LPS, is detrimental for neurogenesis (Ekdahl et al., 2003a; Monje et al., 2003). In contrast, later studies indicated a beneficial effect on neurogenesis of microglia activated by adrenalectomy (Battista et al., 2006), cytokines (Butovsky et al., 2006) or enriched environment (Ziv et al., 2006), but not by physical exercise (Olah et al., 2008). However, we propose a novel role for microglia in the normal, healthy adult neurogenic niche that is independent from the state of activation of the microglial cell and on the level of neurogenesis.

Experimental Procedures

Animals

Wild type (C57BL/6) or transgenic nestin-GFP (Mignone et al., 2004), nestin-CFPNuc (Encinas et al., 2006), fms-EGFP (Sasmono et al., 2003), POMC-EGFP (Overstreet et al., 2004), or hGFAP-GFP (Zhuo et al., 1997) mice were used. All mouse studies were approved by the Baylor College of Medicine Institutional Animal Care and Use Committee and performed in accordance with institutional and federal guidelines.

Histology

Mice were transcardially perfused with saline and 50ml of 4% paraformaldehyde. The brains were dissected out and sectioned with a vibratome. For immunofluorescence, free-floating sections were immunolabeled following conventional procedures (Sierra et al., 2007). For ultrastructural analysis, pre-embedding was used (Encinas and Enikolopov, 2008).

Confocal and electron microscopy

Sections were imaged using a Zeiss LSM or a Leica SP5 confocal microscope. The number of apoptotic cells and/or BrdU+cells per z-stack was estimated using the optical dissector method (Encinas and Enikolopov, 2008). Blind analysis was performed using AxioVision 4.5 (Zeiss) or LAS AF Lite (Leica) and 3D rendering was performed using ImageSurfer (www.imagesurfer.org). For electron microscopy, sections were imaged in a FEI BioIwinG2 Transmission Electron Microscope.

Statistics

Statistical analysis was performed using SPSS. Experiments involving 2 groups were compared using un-paired Student t-test. Experiments involving more than 2 groups were compared by multiple-way Analysis of Variance (ANOVA), followed by post-hoc analysis with LSD (Least Significant Difference). Significance was defined as $p<0.05$. The clearance time was calculated as the percentage of apoptotic BrdU+ cells over the total BrdU+ cells that disappeared between two consecutive points, multiplied by the time in hours between those two points (Barres et al., 1992).

Highlights

- Majority of the SGZ newborn cells enter apoptosis during the first 1–4 days of cell life
- Apoptotic debris is rapidly phagocytosed by unchallenged microglia
- Microglial phagocytic efficiency remains unaffected by increase in age and during inflammation

Lay summary

We report on a critical period of the newborn cell survival, which occurs during the first days of cell life in the adult hippocampus. Apoptotic cells are rapidly phagocytosed by

highly efficient, unchallenged microglia. Apoptosis and phagocytosis are intrinsically coupled, and together, provide potential therapeutic targets for future research in animal models of disease.

Supplementary Material

Refer to Web version on PubMed Central for supplementary material.

Acknowledgments

We would like to thank all the members of the Maletic-Savatic lab for discussion and Fuguo Zhou for technical assistance. We would like to thank Drs. Huda Zoghbi, Juan Botas, Thomas Zwaka, Zhou Zhang, John Swan, Katrina Gwinn, and Vicky Brandt for their critical comments. This work was supported by the National Institute of Neurological Disorders and Stroke (R21NS05875-1 and K08NS0044276), Phillip R. Dodge Young Investigator Award (Child Neurology Society); U.S. Army Medical Research Grant (DAMD170110754) NIH Intellectual and Developmental Disabilities Research Grant (P30HD024064) and the Farish foundation (M.M.-S.). JME is the recipient of a National Alliance for Research on Schizophrenia and Depression Young Investigator Award.

Abbreviations

act-casp3	activated caspase 3
APPO	apposition
BrdU	5-bromo-2′-deoxyuridine
CldU	5-Chloro-2′-deoxyuridine
CFP	cyan fluorescent protein
DAPI	4′,6-Diamidino-2-phenylindole dihydrochloride
dpi	days post-injection
EGFP	enhanced green fluorescent protein
end	endothelial cell
GFAP	glial fibrillary acidic protein
IdU	5-Iodo-2′-deoxyuridine
Iba1	ionized calcium binding adaptor molecule 1
LPS	Salmonella typhimurium lipopolysaccharides
MBP	myelin basic protein
NB	neuroblast
NMDA	N-methyl-D-aspartate
NeuN	neuronal nuclei
ND	non-detectable
NPC	neuroprogenitor cells
ns	non-significant

Ph-index	phagocytic index
PSA-NCAM	Poly-Sialated Neural Cell Adhesion Molecule
pyk	pyknotic
SGZ	subgranular zone
TNG	tangential

References

Ajami B, Bennett JL, Krieger C, Tetzlaff W, Rossi FM. Local self-renewal can sustain CNS microglia maintenance and function throughout adult life. Nat Neurosci. 2007; 10:1538–1543. [PubMed: 18026097]

Aldskogius H, Liu L, Svensson M. Glial responses to synaptic damage and plasticity. J Neurosci Res. 1999; 58:33–41. [PubMed: 10491570]

Aloisi, F. Cytokine production. Neuroglia, HR.; Kettenmann, BR., editors. New York: Oxford UP; 2005. p. 285-301.

Barres BA, Hart IK, Coles HS, Burne JF, Voyvodic JT, Richardson WD, Raff MC. Cell death and control of cell survival in the oligodendrocyte lineage. Cell. 1992; 70:31–46. [PubMed: 1623522]

Battista D, Ferrari CC, Gage FH, Pitossi FJ. Neurogenic niche modulation by activated microglia: transforming growth factor beta increases neurogenesis in the adult dentate gyrus. Eur J Neurosci. 2006; 23:83–93. [PubMed: 16420418]

Biebl M, Cooper CM, Winkler J, Kuhn HG. Analysis of neurogenesis and programmed cell death reveals a self-renewing capacity in the adult rat brain. Neurosci Lett. 2000; 291:17–20. [PubMed: 10962143]

Butovsky O, Ziv Y, Schwartz A, Landa G, Talpalar AE, Pluchino S, Martino G, Schwartz M. Microglia activated by IL-4 or IFN-gamma differentially induce neurogenesis and oligodendrogenesis from adult stem/progenitor cells. Mol Cell Neurosci. 2006; 31:149–160. [PubMed: 16297637]

Davalos D, Grutzendler J, Yang G, Kim JV, Zuo Y, Jung S, Littman DR, Dustin ML, Gan WB. ATP mediates rapid microglial response to local brain injury in vivo. Nat Neurosci. 2005; 8:752–758. [PubMed: 15895084]

Dayer AG, Ford AA, Cleaver KM, Yassaee M, Cameron HA. Short-term and long-term survival of new neurons in the rat dentate gyrus. J Comp Neurol. 2003; 460:563–572. [PubMed: 12717714]

de la Rosa EJ, de Pablo F. Cell death in early neural development: beyond the neurotrophic theory. Trends Neurosci. 2000; 23:454–458. [PubMed: 11006461]

Eid T, Williamson A, Lee TS, Petroff OA, de Lanerolle NC. Glutamate and astrocytes--key players in human mesial temporal lobe epilepsy? Epilepsia. 2008; 49(Suppl 2):42–52. [PubMed: 18226171]

Ekdahl CT, Claasen JH, Bonde S, Kokaia Z, Lindvall O. Inflammation is detrimental for neurogenesis in adult brain. Proc Natl Acad Sci U S A. 2003a; 100:13632–13637. [PubMed: 14581618]

Ekdahl CT, Kokaia Z, Lindvall O. Brain inflammation and adult neurogenesis: the dual role of microglia. Neuroscience. 2009; 158:1021–1029. [PubMed: 18662748]

Ekdahl CT, Mohapel P, Elmer E, Lindvall O. Caspase inhibitors increase short-term survival of progenitor-cell progeny in the adult rat dentate gyrus following status epilepticus. Eur J Neurosci. 2001; 14:937–945. [PubMed: 11595032]

Ekdahl CT, Mohapel P, Weber E, Bahr B, Blomgren K, Lindvall O. Caspase-mediated death of newly formed neurons in the adult rat dentate gyrus following status epilepticus. Eur J Neurosci. 2002; 16:1463–1471. [PubMed: 12405959]

Ekdahl CT, Zhu C, Bonde S, Bahr BA, Blomgren K, Lindvall O. Death mechanisms in status epilepticus-generated neurons and effects of additional seizures on their survival. Neurobiol Dis. 2003b; 14:513–523. [PubMed: 14678767]

Encinas JM, Enikolopov G. Identifying and quantitating neural stem and progenitor cells in the adult brain. Methods Cell Biol. 2008; 85:243–272. [PubMed: 18155466]

Encinas JM, Vaahtokari A, Enikolopov G. Fluoxetine targets early progenitor cells in the adult brain. Proc Natl Acad Sci U S A. 2006; 103:8233–8238. [PubMed: 16702546]

Hatzold J, Conradt B. Control of apoptosis by asymmetric cell division. PLoS Biol. 2008; 6:e84. [PubMed: 18399720]

Hayes NL, Nowakowski RS. Dynamics of cell proliferation in the adult dentate gyrus of two inbred strains of mice. Brain Res Dev Brain Res. 2002; 134:77–85.

Kempermann G, Jessberger S, Steiner B, Kronenberg G. Milestones of neuronal development in the adult hippocampus. Trends Neurosci. 2004; 27:447–452. [PubMed: 15271491]

Kettenmann H. Neuroscience: the brain's garbage men. Nature. 2007; 446:987–989. [PubMed: 17410127]

Kronenberg G, Reuter K, Steiner B, Brandt MD, Jessberger S, Yamaguchi M, Kempermann G. Subpopulations of proliferating cells of the adult hippocampus respond differently to physiologic neurogenic stimuli. J Comp Neurol. 2003; 467:455–463. [PubMed: 14624480]

Kuhn HG, Biebl M, Wilhelm D, Li M, Friedlander RM, Winkler J. Increased generation of granule cells in adult Bcl-2-overexpressing mice: a role for cell death during continued hippocampal neurogenesis. Eur J Neurosci. 2005; 22:1907–1915. [PubMed: 16262630]

Kuhn HG, Dickinson-Anson H, Gage FH. Neurogenesis in the dentate gyrus of the adult rat: age-related decrease of neuronal progenitor proliferation. J Neurosci. 1996; 16:2027–2033. [PubMed: 8604047]

Lagace DC, Whitman MC, Noonan MA, Ables JL, DeCarolis NA, Arguello AA, Donovan MH, Fischer SJ, Farnbauch LA, Beech RD, et al. Dynamic contribution of nestin-expressing stem cells to adult neurogenesis. J Neurosci. 2007; 27:12623–12629. [PubMed: 18003841]

Ma DK, Kim WR, Ming GL, Song H. Activity-dependent extrinsic regulation of adult olfactory bulb and hippocampal neurogenesis. Ann N Y Acad Sci. 2009; 1170:664–673. [PubMed: 19686209]

Mallat M, Marin-Teva JL, Cheret C. Phagocytosis in the developing CNS: more than clearing the corpses. Curr Opin Neurobiol. 2005; 15:101–107. [PubMed: 15721751]

Mandyam CD, Harburg GC, Eisch AJ. Determination of key aspects of precursor cell proliferation, cell cycle length and kinetics in the adult mouse subgranular zone. Neuroscience. 2007; 146:108–122. [PubMed: 17307295]

Marin-Teva JL, Dusart I, Colin C, Gervais A, van Rooijen N, Mallat M. Microglia promote the death of developing Purkinje cells. Neuron. 2004; 41:535–547. [PubMed: 14980203]

Mignone JL, Kukekov V, Chiang AS, Steindler D, Enikolopov G. Neural stem and progenitor cells in nestin-GFP transgenic mice. J Comp Neurol. 2004; 469:311–324. [PubMed: 14730584]

Monje ML, Toda H, Palmer TD. Inflammatory blockade restores adult hippocampal neurogenesis. Science. 2003; 302:1760–1765. [PubMed: 14615545]

Nacher J, McEwen BS. The role of N-methyl-D-asparate receptors in neurogenesis. Hippocampus. 2006; 16:267–270. [PubMed: 16425227]

Neumann H, Kotter MR, Franklin RJ. Debris clearance by microglia: an essential link between degeneration and regeneration. Brain. 2009; 132:288–295. [PubMed: 18567623]

Nicholson DW, Ali A, Thornberry NA, Vaillancourt JP, Ding CK, Gallant M, Gareau Y, Griffin PR, Labelle M, Lazebnik YA, et al. Identification and inhibition of the ICE/CED-3 protease necessary for mammalian apoptosis. Nature. 1995; 376:37–43. [PubMed: 7596430]

Olah M, Ping G, De Haas AH, Brouwer N, Meerlo P, Van Der Zee EA, Biber K, Boddeke HW. Enhanced hippocampal neurogenesis in the absence of microglia T cell interaction and microglia activation in the murine running wheel model. Glia. 2008

Overstreet LS, Hentges ST, Bumaschny VF, de Souza FS, Smart JL, Santangelo AM, Low MJ, Westbrook GL, Rubinstein M. A transgenic marker for newly born granule cells in dentate gyrus. J Neurosci. 2004; 24:3251–3259. [PubMed: 15056704]

Petersen MA, Dailey ME. Diverse microglial motility behaviors during clearance of dead cells in hippocampal slices. Glia. 2004; 46:195–206. [PubMed: 15042586]

Petreanu L, Alvarez-Buylla A. Maturation and death of adult-born olfactory bulb granule neurons: role of olfaction. J Neurosci. 2002; 22:6106–6113. [PubMed: 12122071]

Sasmono RT, Oceandy D, Pollard JW, Tong W, Pavli P, Wainwright BJ, Ostrowski MC, Himes SR, Hume DA. A macrophage colony-stimulating factor receptor-green fluorescent protein transgene is expressed throughout the mononuclear phagocyte system of the mouse. Blood. 2003; 101:1155–1163. [PubMed: 12393599]

Savill J. Recognition and phagocytosis of cells undergoing apoptosis. Br Med Bull. 1997; 53:491–508. [PubMed: 9374033]

Savill J, Dransfield I, Gregory C, Haslett C. A blast from the past: clearance of apoptotic cells regulates immune responses. Nat Rev Immunol. 2002; 2:965–975. [PubMed: 12461569]

Sierra A, Gottfried-Blackmore AC, McEwen BS, Bulloch K. Microglia derived from aging mice exhibit an altered inflammatory profile. Glia. 2007; 55:412–424. [PubMed: 17203473]

Sun W, Winseck A, Vinsant S, Park OH, Kim H, Oppenheim RW. Programmed cell death of adult-generated hippocampal neurons is mediated by the proapoptotic gene Bax. J Neurosci. 2004; 24:11205–11213. [PubMed: 15590937]

Tashiro A, Sandler VM, Toni N, Zhao C, Gage FH. NMDA-receptor-mediated, cell-specific integration of new neurons in adult dentate gyrus. Nature. 2006; 442:929–933. [PubMed: 16906136]

Thomaidou D, Mione MC, Cavanagh JF, Parnavelas JG. Apoptosis and its relation to the cell cycle in the developing cerebral cortex. J Neurosci. 1997; 17:1075–1085. [PubMed: 8994062]

Weise J, Engelhorn T, Dorfler A, Aker S, Bahr M, Hufnagel A. Expression time course and spatial distribution of activated caspase-3 after experimental status epilepticus: contribution of delayed neuronal cell death to seizure-induced neuronal injury. Neurobiol Dis. 2005; 18:582–590. [PubMed: 15755684]

Yang F, Sun X, Beech W, Teter B, Wu S, Sigel J, Vinters HV, Frautschy SA, Cole GM. Antibody to caspase-cleaved actin detects apoptosis in differentiated neuroblastoma and plaque-associated neurons and microglia in Alzheimer's disease. Am J Pathol. 1998; 152:379–389. [PubMed: 9466564]

Zhao C, Teng EM, Summers RG Jr, Ming GL, Gage FH. Distinct morphological stages of dentate granule neuron maturation in the adult mouse hippocampus. J Neurosci. 2006; 26:3–11. [PubMed: 16399667]

Zhuo L, Sun B, Zhang CL, Fine A, Chiu SY, Messing A. Live astrocytes visualized by green fluorescent protein in transgenic mice. Dev Biol. 1997; 187:36–42. [PubMed: 9224672]

Ziv Y, Ron N, Butovsky O, Landa G, Sudai E, Greenberg N, Cohen H, Kipnis J, Schwartz M. Immune cells contribute to the maintenance of neurogenesis and spatial learning abilities in adulthood. Nat Neurosci. 2006; 9:268–275. [PubMed: 16415867]

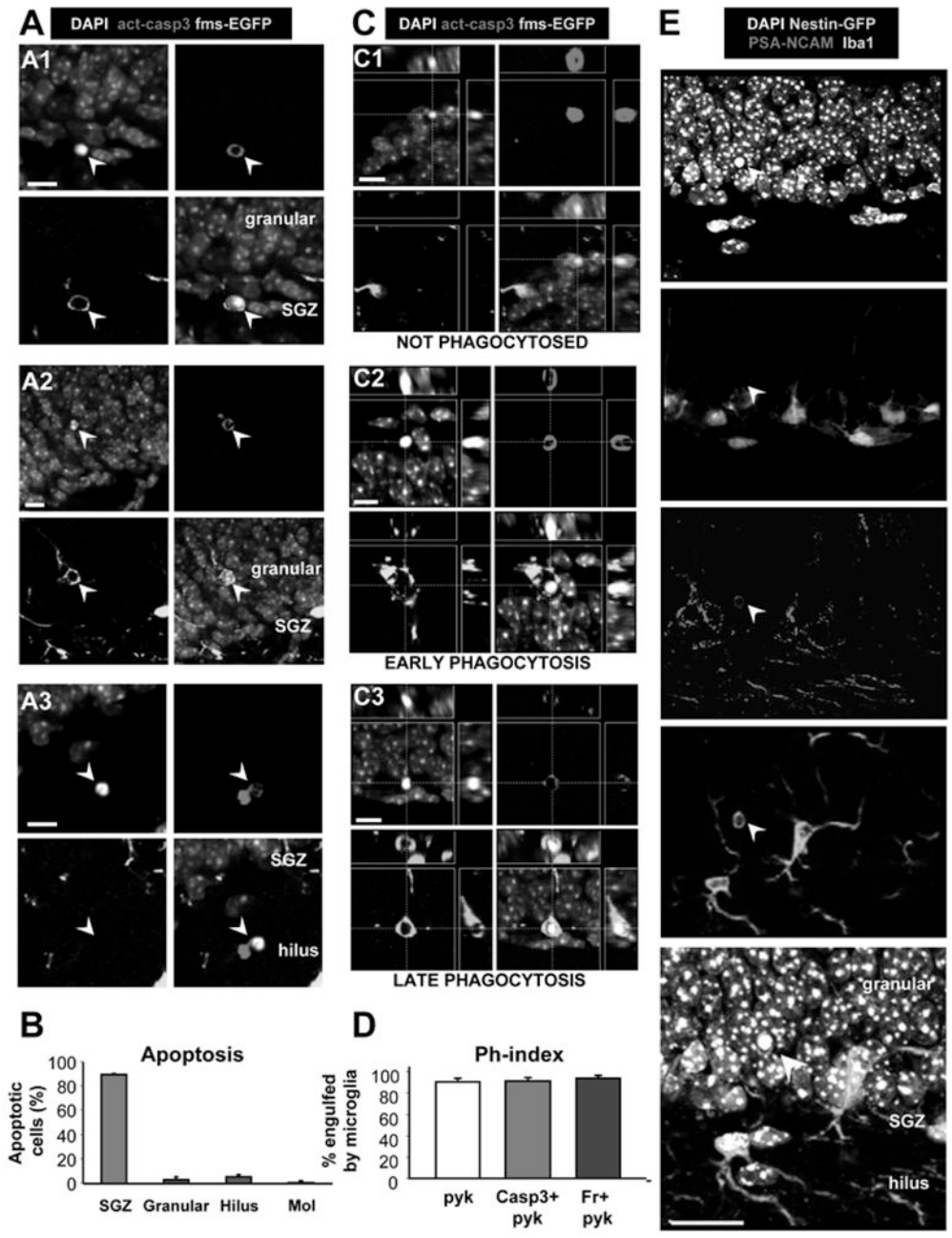

Figure 1. Apoptosis is coupled to phagocytosis in the young adult SGZ

(A) Confocal photomicrographs of apoptotic cells in the young adult (1m.o.) SGZ. Apoptotic cells (arrowheads), detected by pyknosis/karyorrhexis (condensed DAPI staining) and act-casp3, are predominantly located in the SGZ (A1), and more sparsely in the granular cell layer (A2) and hilus (A3). Apoptotic cells in A1 and A2 are engulfed by microglia visualized in fms-EGFP mice.

(B) Quantification of the location of apoptotic cells, identified by pyknosis and act-casp3 expression, in the hippocampus. The vast majority of apoptotic cells is located strictly in the SGZ.

(C) Different stages of phagocytosis in the SGZ. The microglial engulfment of apoptotic cells (pyknotic, act-casp3 immunopositive) was assessed in orthogonal projections of confocal z-stacks. Apoptotic cells are either not phagocytosed (C1);

undergoing early phagocytosis (loose microglial pouch, conspicuous act-casp3 immunolabeling; C2); or late phagocytosis (tight microglial pouch, dim act-casp3 immunolabeling; C3).

(D) Quantification of the phagocytic index (Ph-index), i.e., the percentage of SGZ apoptotic cells that are engulfed by microglia (early and late phagocytosis together), in three independent experiments. A large percentage (> 90%) of the apoptotic cells is completely engulfed by microglia.

(E) Confocal photomicrographs of the SGZ showing Iba+ microglial processes and somas intermingled with the SGZ NPCs (nestin-GFP+) and NBs (PSA-NCAM+). DAPI staining indicates cell nuclei. The arrowhead points to an apoptotic (pyknotic) cell, identified by condensed DAPI staining, that expresses PSA-NCAM and is engulfed by the microglial process.

Scale bars: A, C, 10μm; E, 20μm; See also Fig. S1. Bars represent mean ± SEM

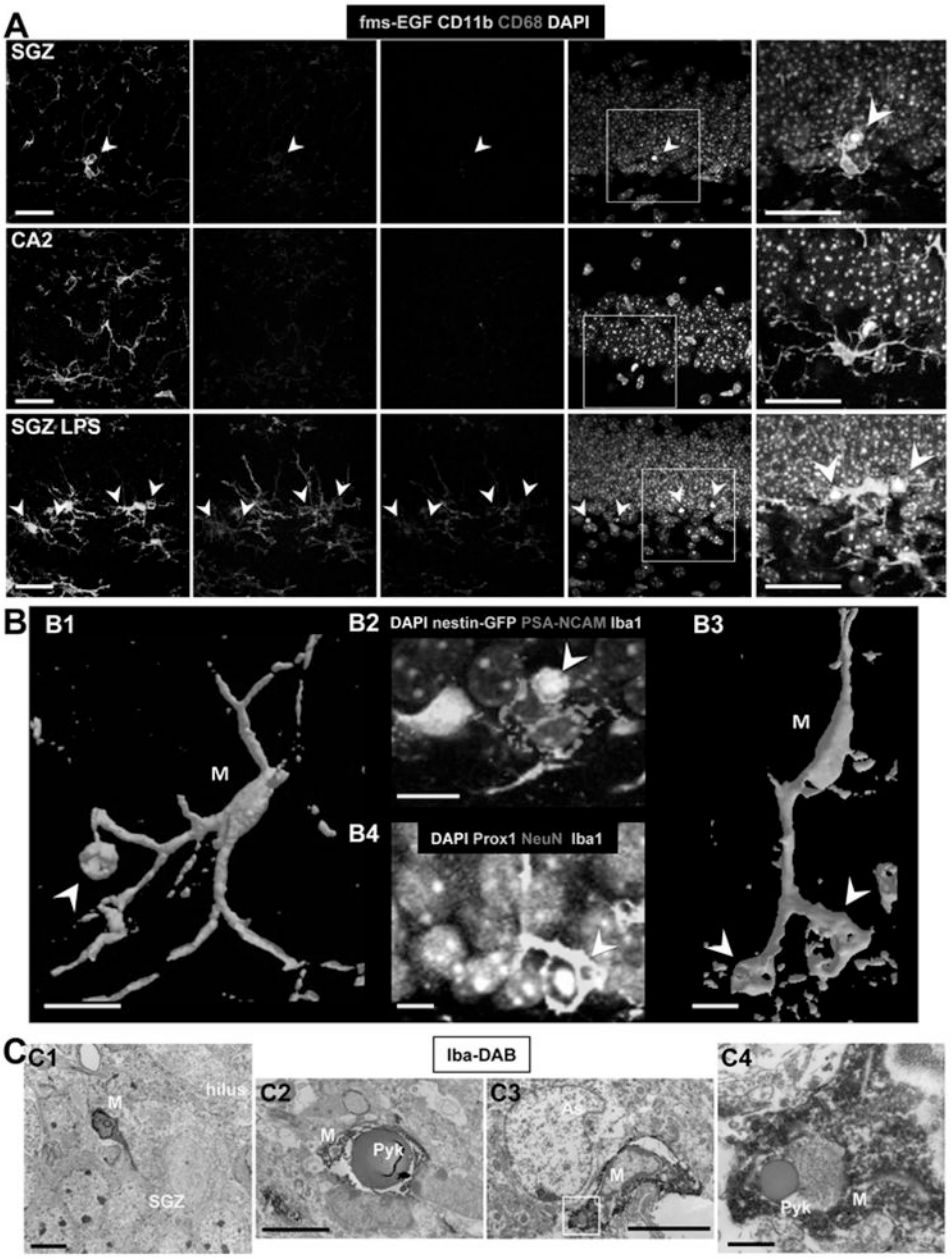

Figure 2. Unchallenged microglia phagocytose a*poptotic cells in the normal adult SGZ*

(A) Confocal photomicrographs of the expression of CD11b and CD68 in phagocytic microglia. Phagocytic SGZ and non-phagocytic CA2 microglia express low levels of CD11b and CD68, while LPS-challenged microglia express high levels of these markers (n=3 fms-EGFP mice; LPS 5mg/kg, 24h). The expression of fms-EGFP is similar in all experimental groups studied. Identical confocal settings were used to collect images from all animals. Enlarged insets of the merged images are shown at the end of each row. See also Fig. S2.

(B) Phagocytosis by microglia involves a ball-and-chain structure, formed by microglial *en passant* or terminal branches clearly distinguishable from the microglial cell body (M), as shown in volume rendering images of confocal z-stacks. The microglial phagocytic pouch in B1 (arrowhead) is shown in detail in B2: a pyknotic nucleus located on top of a PSA-NCAM+ NB and nearby nestin-GFP+ NPC is undergoing phagocytosis. The right microglial phagocytic pouch in B3 (arrowhead) is shown in

detail in B4: a pyknotic nucleus located amongst immature and mature neurons (labeled with Prox1 and NeuN, respectively) is undergoing phagocytosis.

(C) Electron micrographs of the apoptotic cells and phagocytosis by microglia in the young adult SGZ. C1, Microglia (M), detected by Iba1-DAB immunostaining, is intermingled among the SGZ cells; C2, apoptotic cell (Pyk), identified by nuclear morphology, is engulfed by microglia (M); C3, terminal apoptotic debris is engulfed by microglia (M). C4, enlarged region of interest from C3.

Scale bars: A, 20μm (z=10μm); B, 10μm; C1-C3, 5μm; C4, 500nm. Arrowheads, phagocytic pouches; M, microglia; h, hilus; Pyk, pyknotic body; As, astrocyte.

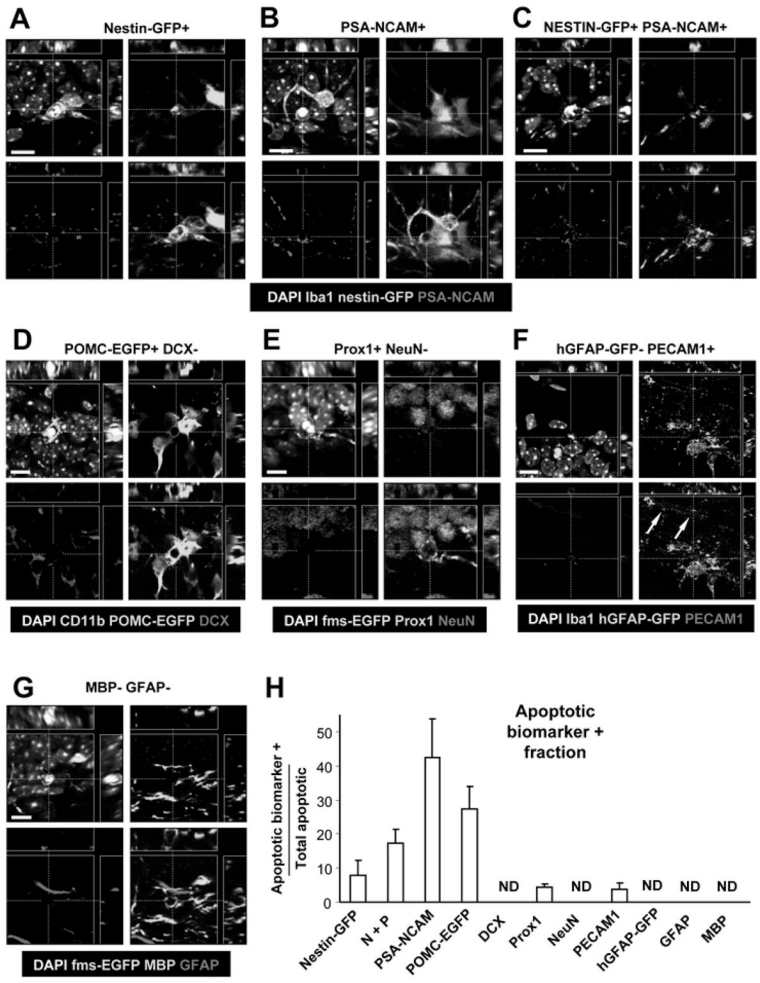

Figure 3. Cell identity of the SGZ apoptotic cells

Confocal orthogonal projections of apoptotic cells, identified by pyknosis/karyorrhexis, express different cell-type specific biomarkers in the young adult neurogenic SGZ. Low magnification images of all immunolabeling data can be found in Fig. S3.

(A) Apoptotic cell expressing nestin-GFP.

(B) Apoptotic cell expressing PSA-NCAM.

(C) Apoptotic cell expressing nestin-GFP and PSA-NCAM.

(D) Apoptotic cell expressing POMC-EGFP but not DCX.

(E) Apoptotic cell expressing Prox1 but not NeuN.

(F) Apoptotic cell expressing PECAM1 but not hGFAP-GFP. A capillary with PECAM1+ endothelial cell surrounded by hGFAP-GFP+ astrocytic terminal feet is nearby (arrows).

(G) Apoptotic cell not expressing either MBP or GFAP.

(H) Fraction of SGZ apoptotic cells expressing each of the different cell-type markers shown above. The majority of the apoptotic cells expresses markers of cells found in early stages of the neurogenic cascade.

Scale bars: 10μm. ND, non-detectable. Bars represent mean ± SEM. Arrows, capillary.

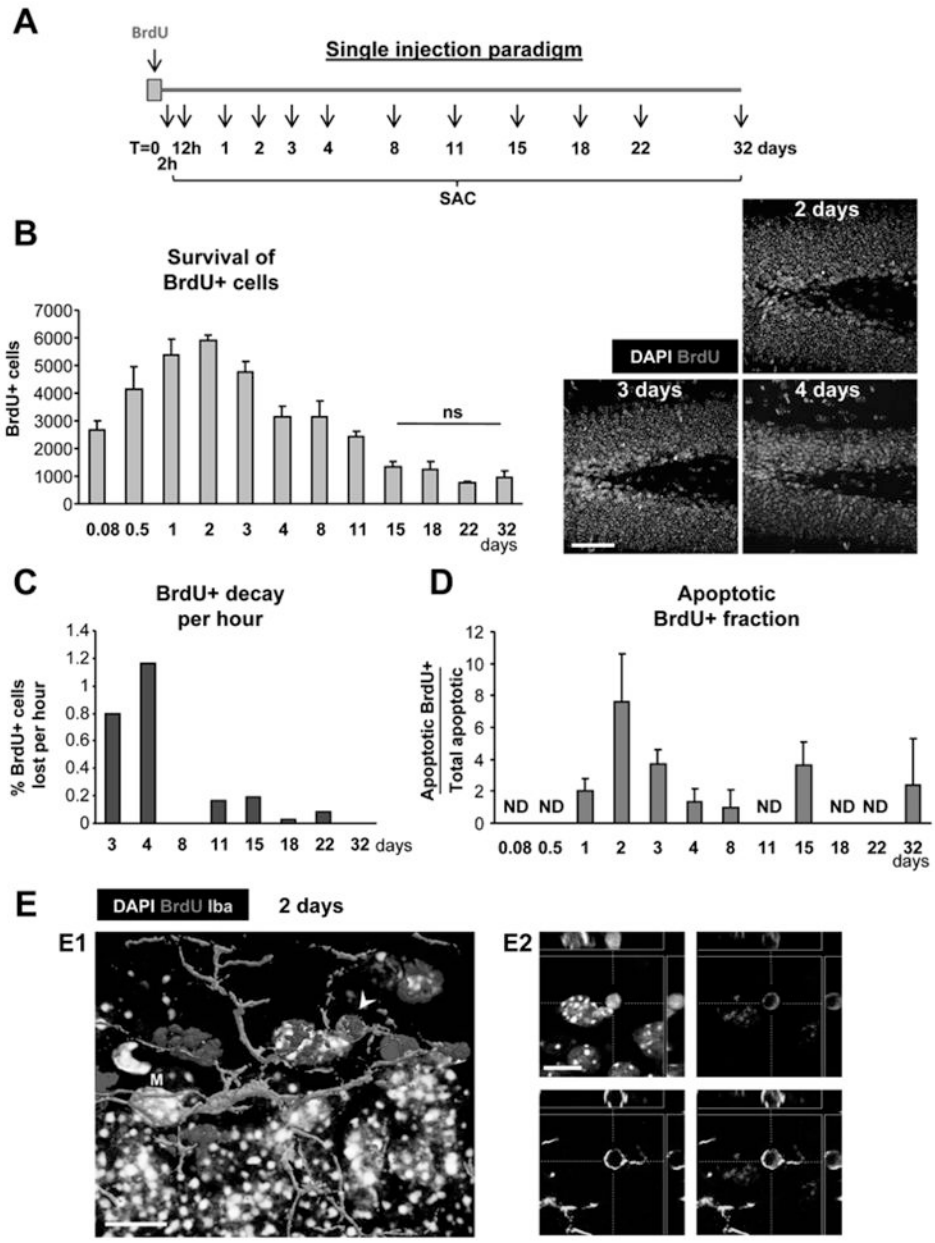

Figure 4. Survival of newborn cells in a single BrdU injection paradigm

(A) Experimental design showing a single injection of BrdU at t=0 and the different time points studied thereafter (SAC = sacrifice time points).

(B) Left panel: quantification of the number of BrdU+ cells along the time course of 32 days post-injection (dpi). Statistical differences were assessed by ANOVA ($p<0.001$) followed by Least Significant Difference (LSD) tests comparing each time point with all later time points. The maximum number is reached at 2 dpi and decreases afterwards. Starting from 15 dpi, no significant differences are found with any of the later time points (ns). Right panel: Photomicrographs of the 1 m.o. mouse sections of the dentate gyrus at 2, 3 and 4 dpi depict the decrease in the number of BrdU+ cells in the SGZ.

(C) BrdU decay, quantified as percentage of the cells at 2 dpi lost per hour.

(D) Apoptotic BrdU+ fraction, quantified as the percentage of apoptotic cells labeled with BrdU along the time course of 32 dpi. Apoptotic BrdU+ cells are mostly found between 1 and 3 dpi.

(E) Confocal photomicrograph of an apoptotic (pyknotic) cell labeled with BrdU at 2 dpi (arrowhead) and phagocytosed by microglia (M), shown as a three-dimensional rendering (E1) and in orthogonal projections of confocal z-stacks (E2). (Same cell is shown in Fig. S1E).

Scale bars: B, 50μm (z=20μm); E1, E2, 10μm. ND, non-detectable. Bars represent mean ± SEM.

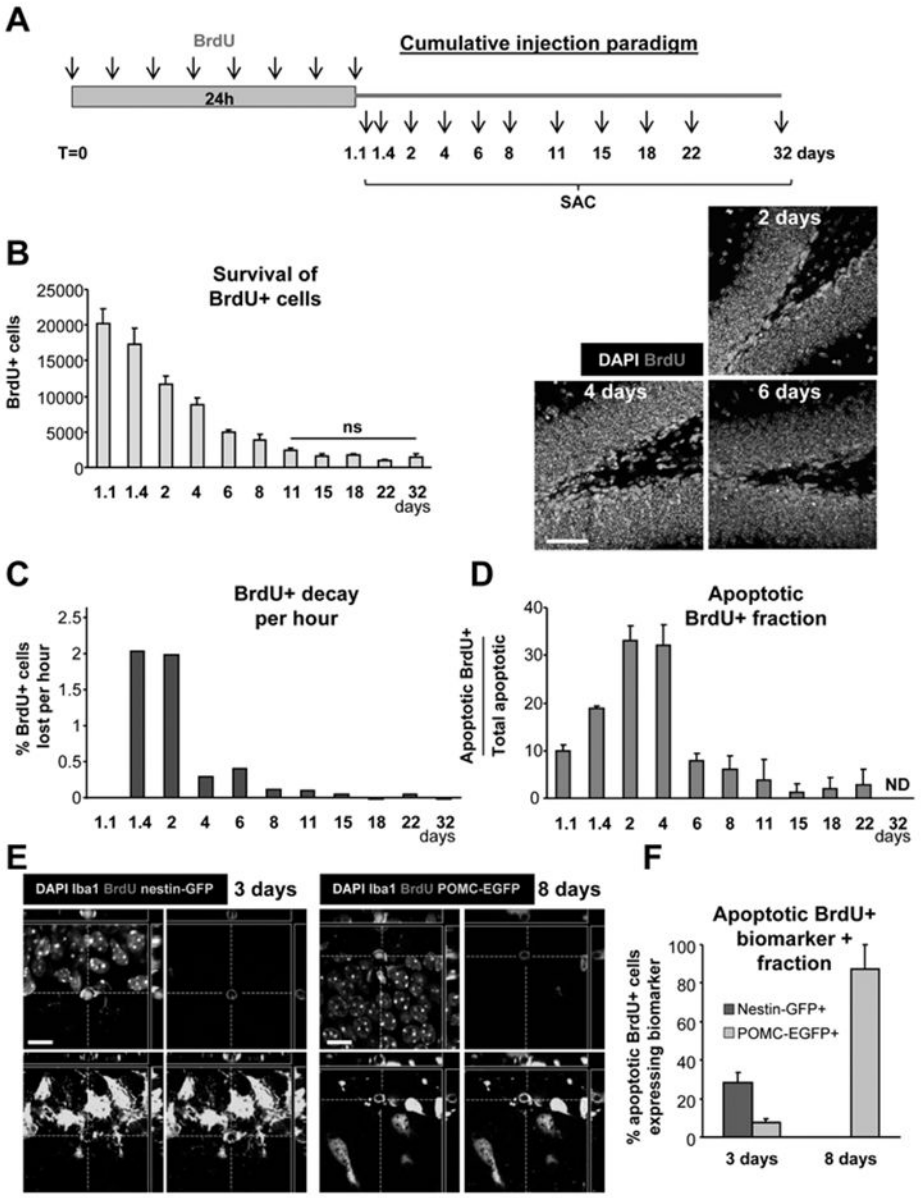

Figure 5. Survival of newborn cells in a cumulative BrdU injection paradigm

(A) Experimental design showing the injection of BrdU every 3h for 24h and the different time points studied after the first injection (SAC = sacrifice time points).

(B) Left panel: quantification of the number of BrdU+ cells along the time course of 32 days post-injection (dpi). Statistical differences were assessed by ANOVA ($p<0.001$) followed by LSD tests comparing each time point with all later time points. Starting from 11dpi, no significant differences are found with any of the later time points (ns). Right panel: Photomicrographs of the 1 m.o. mouse sections of the dentate gyrus at 2, 4 and 6 dpi depict larger number of BrdU+ cells labeled with the cumulative BrdU paradigm compared to the single BrdU paradigm, but still decreasing in number over time.

(C) BrdU decay, quantified as percentage of the cells at 2 dpi lost per hour.

(D) Apoptotic BrdU+ fraction, quantified as the percentage of apoptotic cells labeled with BrdU along the time course of 32 dpi. Apoptotic BrdU+ cells peak between 2 and 4dpi.

(E) Confocal photomicrographs of the nestin-GFP and POMC-EGFP expression in the early (3dpi) and late (8dpi) critical periods, respectively.

(F) Quantification of the biomarker expression in the early (3dpi) and late (8dpi) critical periods. In the early critical period, apoptotic cells express nestin-GFP and POMC-EGFP, whereas only POMC-EGFP is expressed in the late critical period. Scale bars: B, 50μm (z=20μm); E, 10μm. ND, non-detectable. Bars represent mean ± SEM. See also Fig. S4.

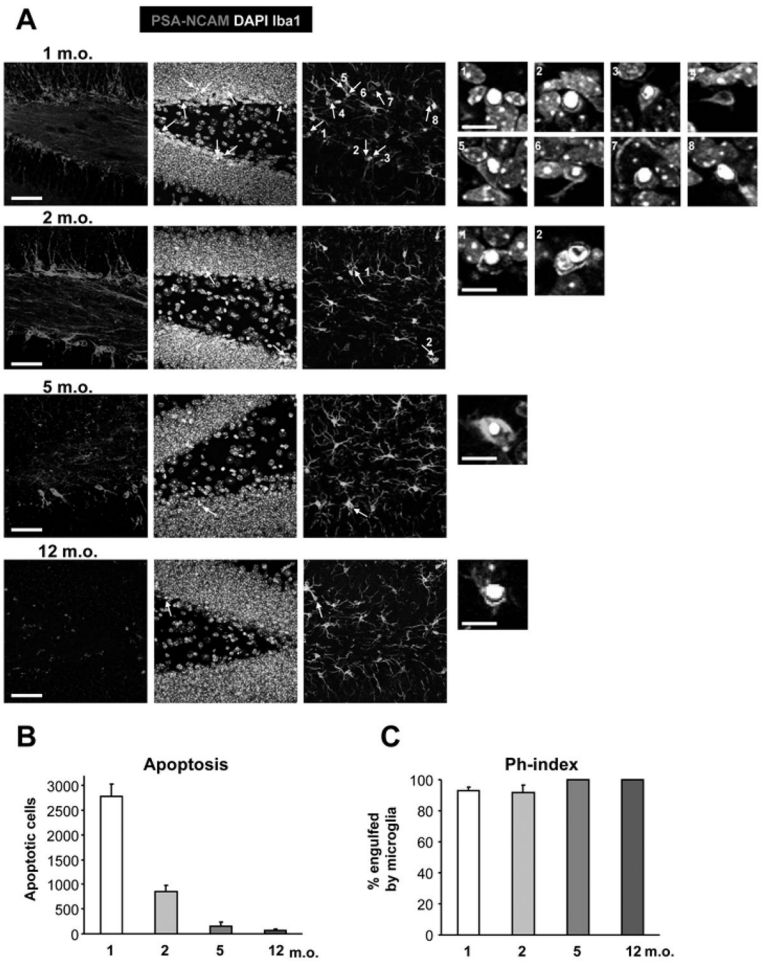

Figure 6. Age-dependent decline in SGZ apoptosis

(A) Photomicrographs of the hippocampal sections obtained from 1, 2, 5, and 12 m.o. mouse demonstrate the decline in the number of NBs (PSA-NCAM+) and the number of apoptotic profiles, identified by nuclear morphology (pyknosis) and phagocytosis by microglia (Iba1+), pointed by arrows. Numbered insights represent higher magnification of the identified apoptotic cells.

(B) Quantification of the number of apoptotic cells in the SGZ during adulthood. The number of SGZ apoptotic cells decreases sharply after 1 month of age.

(C) Quantification of the Ph-index. The microglial phagocytic efficiency remains constant throughout adulthood.

Scale bars; low magnification, 50μm (z=16.24μm); high magnification, 10μm. Bars represent mean ± SEM.

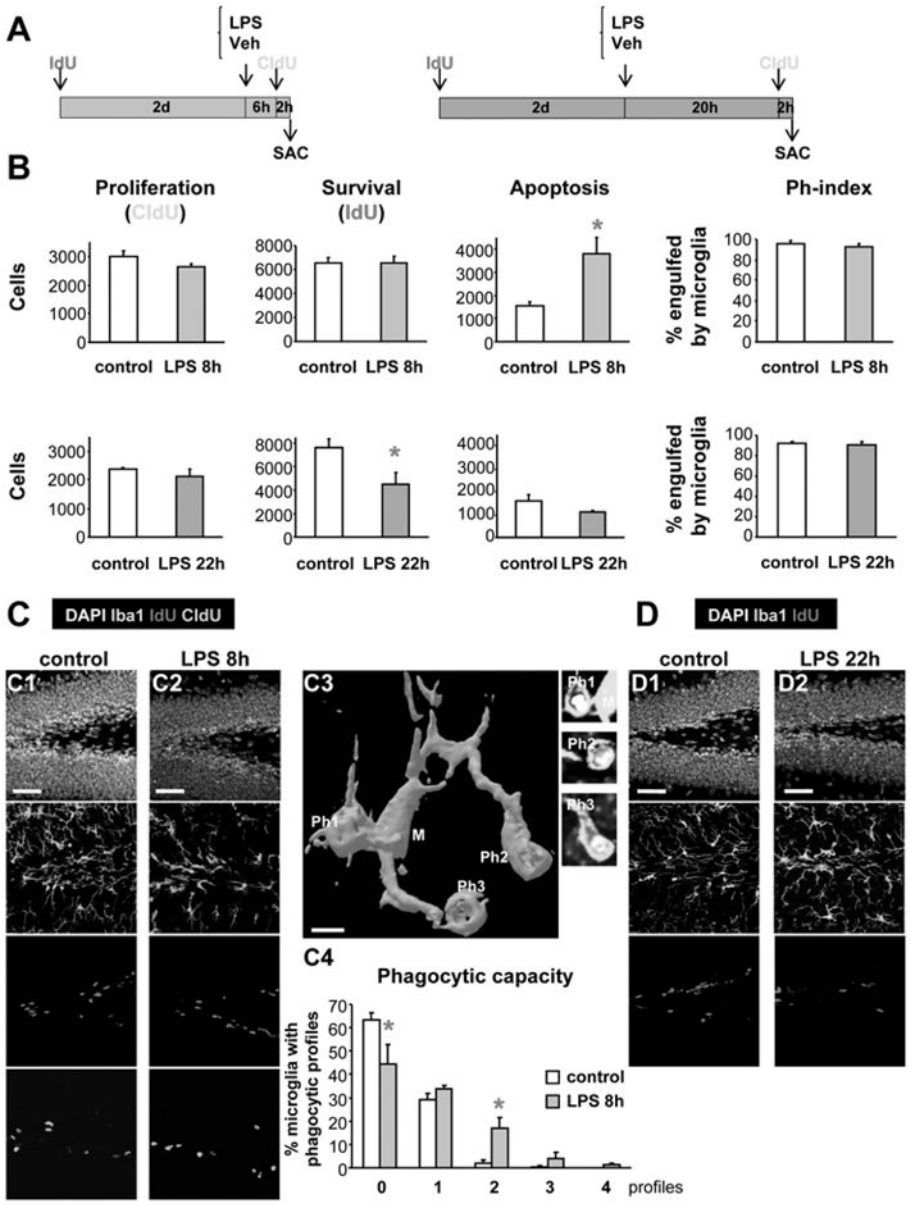

Figure 7. Acute inflammation affects young adult SGZ neurogenesis and apoptosis

(A) Experimental paradigm for the study of the effects of LPS (1mg/kg), 8h or 22h, on the neurogenic cascade. To study the LPS effect on newborn cell survival, IdU was injected 2 days before LPS. To study the LPS effect on cell proliferation, CldU was injected 2 hr before the end of the experiment (SAC = sacrifice time points).

(B) Quantification of the effects of LPS 8h (upper panels) or 22h (lower panels) after treatment, on the NPC proliferation (CldU + cells), newborn cell survival (IdU+ cells), apoptosis (pyknosis), and Ph-index. SGZ apoptosis increases 8h after LPS and is followed by a decreased survival 22h after LPS. Proliferation and Ph-index remain unaffected.

(C) Representative examples of the proliferation, survival, apoptosis and phagocytosis in the young adult mouse SGZ in control and LPS-treated animals at 8h (C1, C2). A 3D rendering of a microglial cell (8h after LPS) phagocytosing three apoptotic cells is shown in C3. The phagocytic capacity (percentage of microglia with 0–4 phagocytic profiles) is increased 8h after LPS treatment (C4).

(D) Representative examples of the proliferation, apoptosis and phagocytosis in the young adult mouse SGZ in control and LPS-treated animals at 22 hours (D1, D2). See also Fig. S5.

Scale bars: C1, C2, 50μm (z=20μm); C3, 5μm; D1, 2, 50μm (z=20μm). Ph1-3, phagocytic processes. Bars represent mean ± SEM.*, $p<0.05$ (Student t-test).